Scientific Research Publishing

Open Journal of Applied Sciences, 2023, 13, 2343-2359
https://www.scirp.org/journal/ojapps
ISSN Online: 2165-3925
ISSN Print: 2165-3917

Analysis and Simulation of the Influence of Electromagnetic Fields on Living Beings near HV Power Lines Using the FDTD Method

Anthony Bassesuka Sandoka Nzao

ISTA Kinshasa, Electrical Engineering, Kinshasa, The Democratic Republic of the Congo
Email: bass_sandoka@yahoo.fr

How to cite this paper: Nzao, A.B.S. (2023) Analysis and Simulation of the Influence of Electromagnetic Fields on Living Beings near HV Power Lines Using the FDTD Method. *Open Journal of Applied Sciences*, **13**, 2343-2359.
https://doi.org/10.4236/ojapps.2023.1312183

Received: November 17, 2023
Accepted: December 17, 2023
Published: December 20, 2023

Abstract

Recent decades have seen rapid advances in the field of electrical engineering, such that our environment has become a sea of electrical and magnetic signals, raising questions about the possible effects of low-frequency electromagnetic fields on the environment and which are capable of modifying and destroying our ecosystem. Particular interest was given in this article due to a massive influx of population living near high voltage lines. The analysis and simulation of the influence of low frequency electromagnetic fields on living beings in the vicinity of high voltage sources 132 kV and 220 kV in urban areas in DR Congo is the subject of our research with a view to estimating the level of exposure of humans to low frequency electromagnetic fields. To carry out our research, we used the classic method of analyzing the field produced near a high voltage line based on Maxwell's image theory, the Maxwell-Gauss theorem and Maxwell-Ampère theorem to model and quantify low-frequency electromagnetic fields in the vicinity of high-voltage lines. The 2D FDTD numerical formulation was developed from telegraphers' equations and allowed us to obtain models of current and voltage induced by electromagnetic fields on living beings below and near HV lines. The different simulations carried out on the proposed models illustrate the effects of the electrical and geometric parameters of the pylons on the distribution of the electromagnetic field in the vicinity of the HV lines. The results obtained were compared to the safety limits recommended by the standards.

Keywords

Low Frequency Electromagnetic Field, Modeling, Field and Health, Maxwell's Equations, FDTD Method, Electromagnetic Compatibility, High Voltage Line

1. Introduction

On a daily basis, we are constantly exposed to electromagnetic fields of natural, but also artificial, origin. These result from the ever-increasing use of electrical energy and raise questions about the possible effects of exposure to these fields on human health. The influence of low frequency electromagnetic fields and their interactions with biological tissues cause effects not only on these tissues but also are capable of modifying and destroying our ecosystem [1]. Several attempts have been made to harmonize European standardization relating to exposure to low-frequency electromagnetic fields. In a public report [2], the United States National Academy of Sciences concluded that "the totality of currently available evidence does not demonstrate that residential exposure to electric and magnetic fields at industrial frequency presents a danger to human health". On the other hand, the biological effects due to induced currents are well known. These are reversible effects on humans. Nevertheless, the case of our investigation, several elements of which are demonstrated on the flowcharts, illustrates the extent to which these effects are dangerous for human health but also how the population is exposed due to lack of knowledge and non-compliance with standards [3] [4].

The work published by [5] demonstrates that electromagnetic fields can lead to an increase in the electrical potential of biological tissues; a survey was carried out on people living near the high voltage line, and this demonstrated that there is the potential risks for people exposed to interactions between electromagnetic fields and the human body are real and therefore require protective measures [6]. Exposure to these sources is real and can lead to negative consequences on the environment, especially for living beings near high-voltage power lines and transformers [7]. During our survey, we found that the population was staying longer under and near high-voltage lines without respecting the distance required by the international electrotechnical commission IEC. However, exposure to these electromagnetic fields generates currents within the body, and the corresponding absorption of energy in tissues results in an increase in temperature [8]. The health effects generated are mainly a function of the coupling mechanism, the nature of the fields and the duration of exposure [9]. These phenomena are all the more important as the intensity and/or frequency of the signal are high [6] [10]. In addition to the effects observed on living beings near HV lines which can have an influence on biological functions, electromagnetic fields also act on electronic devices [11]. It is therefore important when constructing a low frequency HV line to ensure that their operation does not disrupt that of other devices or itself fall victim to other sources of electromagnetic fields in order to avoid any form of electromagnetic incompatibility [12]-[17].

The need to quantify and control the level of the electromagnetic field radiated by high voltage devices (HV lines, transformers) in urban areas is essential. Electromagnetic fields being a physical entity difficult to model and interpret, we also considered it useful to proceed by understanding the analytical me-

thod based on the theorems for calculating low frequency electromagnetic fields in order to study and analyze all parameters that could allow us to make a simulation relating to the characterization of the electromagnetic environment generated by HV lines. The classic method of analyzing the field produced near a high voltage line based on Maxwell's image theory, the Maxwell-Gauss theorem and Maxwell-Ampère theorem was used to model and quantify the field low frequency electromagnetics in the vicinity of high voltage lines. This method has many advantages over other methods of calculating the electric field. It does not require integration in the construction of the matrix of coefficients for charges, potentials and currents. Then, it makes it possible to model the electromagnetic environment of a high voltage line using simple algebraic models. This makes programming easier and calculation faster.

In another context, it is also appropriate to use other analytical approaches based on the theorems for calculating low frequency electromagnetic fields such as the charge simulation method [18], the theorems of Biot and Savart as well as the numerical simulation methods for complex geometries, because the scientific literature has proven the effectiveness of numerical methods for solving Maxwell's equations in both the frequency and time domains. Among these most used methods, we can cite the finite element method, the finite difference method, the finite difference method in the time domain (FDTD) as well as the impedance method [19].

The 2D FDTD numerical formulation was developed from telegraphers' equations and allowed us to obtain models of current and voltage induced by electromagnetic fields on living beings below and near HV lines.

Our work aims to complete and reinforce the veracity of some of the results already obtained. The calculations are carried out on the low frequency 132 kV and 220 kV HV lines in Kinshasa in DR Congo. This study was supplemented by a citizen survey carried out among populations living below and near these HV lines to verify the living conditions of these populations exposed to electric and magnetic fields.

The 2D simulations based on the proposed models were presented as well as the verification of the consistency of the different models, by comparing the fractal dimensions of the results of our programs with those of the figures obtained experimentally.

2. Theoretical Model

2.1. Modeling of the Electromagnetic Field in the Vicinity of an HV Line

Within the framework of this article, we used the method of the images of Maxwell [20] based on the theorems of Gauss and Ampère to model the electromagnetic environment generated by the HT lines to compare it with the international standards concerning the exposure of the human being to this type of the field.

2.1.1. Model of the Electric Field

For a line with several phases, as shown in **Figure 1**, the total load q of the line can be determined from the following matrix expression [20] [21]:

$$\frac{1}{2\pi\varepsilon_0}[q]=[P]^{-1}[V]=[M][V] \tag{1}$$

Or: $[q]=[q_1,q_2,q_3,\cdots]$ the column matrix of the loads for the n phases; $[V]=[V_1,V_2,V_3,\cdots,V_n]_t$ the column matrix of phase-to-neutral voltages for the n phases; $[P] = n \times n$ Matrix of potential coefficients, with [20] [21]:

$$P_{ii}=\ln\left(\frac{2H_i}{r_{éq}}\right) \quad \text{and} \quad P_{ij}=\ln\left(\frac{I_{ij}}{A_{ij}}\right), i \neq j \tag{2}$$

With H_i is the average height of conductor I concerning to ground, and this is determined as shown in **Figure 2** by the following expression:

$$H_i = H_{\min} + \frac{f}{3} \tag{3}$$

Consider a three-phase line with bundled conductors, the voltages of the three phases of which are given by the following matrix:

$$[V]=V_m\left[\sin(\omega t+\varphi),\sin(\omega t+\varphi-120^\circ),\sin(\omega t+\varphi+120^\circ)\right] \tag{4}$$

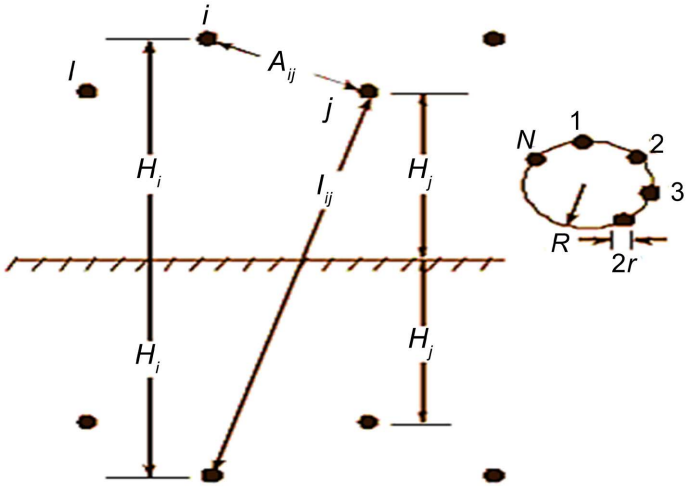

Figure 1. Configuration of an n-phase line for the calculation of the total load [20] [21].

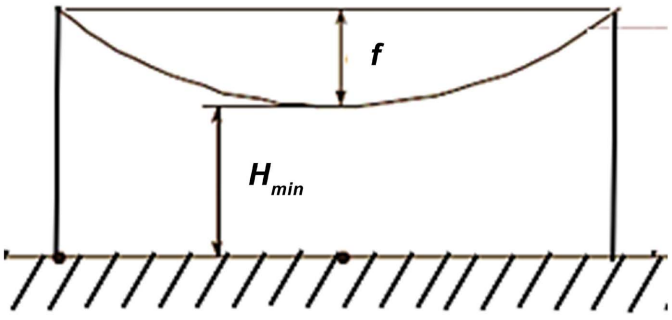

Figure 2. Arrow f of a line between two pylons [20] [21] [22].

In general, one selects an x and y coordinate system that is at ground level below and in the middle of the line, *i.e.* the coordinates of the conductors of the line (x_i, y_i), as shown in Figure 3.

A point (x, y) is represented in Figure 3 to determine the different components (vertical, horizontal, and total) of the electric field E, the vector of the field created by the charge q_i of the conductor:

$$E_c = \frac{q_i}{2\pi\varepsilon_0}\frac{1}{D_i} \tag{5}$$

Or:

$$D_i^2 = \left(x - x_i\right)^2 + \left(y - y_i\right)^2 \tag{6}$$

The vertical and horizontal components (E_h) of E_c are given respectively by the following equations:

$$E_V = E_C \cdot \sin\theta = \frac{q_i}{2\pi\varepsilon_0}\frac{y - y_i}{D_i'} \tag{7}$$

Similarly, the image of the charge q_i with respect to the earth induces at point A:

$$E_C' = E_C = \frac{q_i}{2\pi\varepsilon_0}\frac{1}{D_i'} \tag{8}$$

Or: $\left(D_i'\right)^2 = \left(x - x_i\right)^2 + \left(y + y_i\right)^2$

$$\begin{cases} E_h' = E_C \cdot \cos\theta = \dfrac{q_i}{2\pi\varepsilon_0}\dfrac{x - x_i}{\left(D_i'\right)^2} \\ E_v' = E_C \cdot \sin\theta = \dfrac{q_i}{2\pi\varepsilon_0}\dfrac{y - y_i}{\left(D_i'\right)^2} \end{cases} \tag{9}$$

The total components of the electric field in the horizontal and vertical direction created at point A by the two charges q_i and its image with respect to the earth.

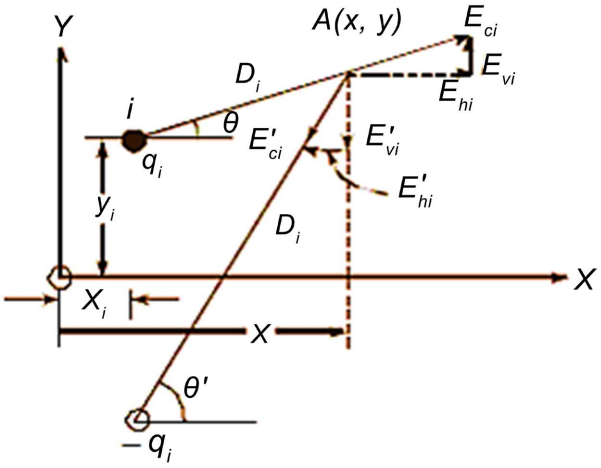

Figure 3. Determination of the electrostatic field in the vicinity of the line [1] [21] [22] [23].

$$E_{hi} = \frac{q_i}{2\pi\varepsilon_0}(x - x_i)\left[\frac{1}{D_i^2} - \frac{1}{(D_i')^2}\right] \tag{10}$$

$$E_{vi} = \frac{q_i}{2\pi\varepsilon_0}\left[(y - y_i)\frac{1}{D_i^2} - (y + y_i)\frac{1}{(D_i')^2}\right] \tag{11}$$

Therefore, for n phases, the sum of the horizontal and vertical components of the fields created at point A. So for a three-phase line we can write, taking:

$$J_i = (x - x_i)\left[\frac{1}{D_i^2} - \frac{1}{(D_i')^2}\right] \tag{12}$$

$$K_i = (y - y_i)\frac{1}{D_i^2} - (y + y_i)\frac{1}{(D_i')^2} \tag{13}$$

Hence, phase 1 creates at point A the total horizontal component E_{hi} given as follows:

$$E_{hi} = \frac{q_i}{2\pi\varepsilon_0} J_i \tag{14}$$

With the load q_i given by formulas (1) and (4), it is shown that, the maximum value of the horizontal component:

$$E_{hm} = J_h \cdot V_m \quad 15)$$

The effective value of the horizontal component of the electric field at point A due to the three phases of the line will be:

$$E_{hm} = J_h \cdot \frac{V_m}{\sqrt{3}} = J_h \cdot V \tag{16}$$

where V is the simple RMS voltage of the line. In the same way, we can determine the effective value of the vertical component E_{vn}:

$$E_{vn} = K_v \cdot V = \sqrt{K_{v1}^2 + K_{v2}^2 + K_{v3}^2 - K_{v1}K_{v2} - K_{v2}K_{v3} - K_{v3}K_{v1}} \tag{17}$$

Or:

$$\begin{cases} K_{v1} = K_1 M_{11} + K_2 M_{21} + K_3 M_{31} \\ K_{v2} = K_1 M_{12} + K_2 M_{22} + K_3 M_{32} \\ K_{v3} = K_1 M_{13} + K_2 M_{23} + K_3 M_{33} \end{cases} \tag{18}$$

where the values of K_1, K_2 and K_3 are obtained from formula (13) for $i = 1, 2, 3$.

2.1.2. Model of the Magnetic Field

The passage of an electric current of intensity "I", in a cylindrical conductor, creates a circular magnetic induction field whose tangential component outside the conductor is given by Ampère's theorem [21] [22] [23]:

$$B = \frac{\mu_0 \cdot i}{2\pi r} \tag{19}$$

Based on Maxwell's image method, we calculate the magnetic field created at any point in space in the vicinity of the line. In most applications, the magnetic

field strength at ground level is the important calculated value. Figure 4(a) represents the three phases of a high voltage line with their images to the ground, "h" is the height of each phase, "S" is the distance between phases, and we place the axis of coordinates x and y on the earth whose origin is at the center of the line. The passage of a current I_c (the current direction e.g. exiting the page) through phase "C" creates at point $P(x, y)$, as shown in Figure 4(b), a magnetic field whose amplitude is calculated as follows:

$$H_C = \frac{I_C}{2\pi D_C} \tag{20}$$

$$D_C = \sqrt{(x-S)^2 + (y-h)^2} \tag{21}$$

The two-component magnetic field vector: horizontal H_{ch} and vertical H_{cv} given by Equations (22) and (23) respectively as follows:

$$H_{Ch} = H_C \cdot \cos\theta_C = -\frac{I_C}{2\pi D_C} \cdot \frac{y-h}{D_C} = -\frac{I_C}{2\pi} \cdot \frac{y-h}{(x-S)^2 + (y-h)^2} \tag{22}$$

$$H_{Cv} = H_C \cdot \sin\theta_C = -\frac{I_C}{2\pi D_C} \cdot \frac{x-S}{D_C} = -\frac{I_C}{2\pi} \cdot \frac{x-S}{(x-S)^2 + (y-h)^2} \tag{23}$$

For the phase image C, create at point P the field H_i (Figure 4(b)).

$$H_i = \frac{I_C}{2\pi D_i} \tag{24}$$

With $D_i = \sqrt{(x-S)^2 + (y+h)^2}$.

Similarly, the horizontal and vertical component of H_i are given by Equations (27) and (28), respectively:

$$H_{ih} = H_i \cdot \cos\theta_i = -\frac{I_C}{2\pi D_i} \cdot \frac{y+h}{D_i} = -\frac{I_C}{2\pi} \cdot \frac{y+h}{(x-S)^2 + (y+h)^2} \tag{25}$$

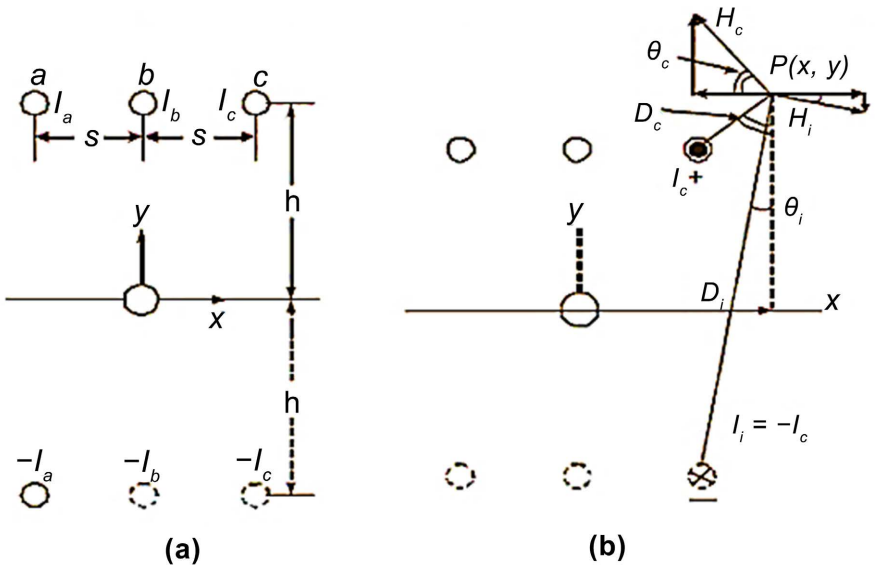

Figure 4. Maxwell's image method [1] [21] [22].

$$H_{vh} = H_i \cdot \sin\theta_i = -\frac{I_C}{2\pi D_i} \cdot \frac{x-S}{D_i} = -\frac{I_C}{2\pi} \cdot \frac{x-S}{(x-S)^2 + (y+h)^2} \tag{26}$$

From Figure 4(b), we see that the horizontal and vertical components of H_i are in the opposite direction to those of H_c. So, in conclusion, that the horizontal and vertical component of the total field H at point P due to the current I_c and its image $I_i = -I_c$ will be given by Equations (27) and (28) respectively:

$$\begin{aligned} H_h &= H_C \cdot \cos\theta_C + H_i \cdot \cos\theta_i \\ &= -\frac{I_C}{2\pi} \cdot \left[\frac{y+h}{(x-S)^2 + (y+h)^2} - \frac{y-h}{(x-S)^2 + (y-h)^2} \right] \end{aligned} \tag{27}$$

$$\begin{aligned} H_v &= H_C \cdot \sin\theta_C + H_i \cdot \sin\theta_i \\ &= -\frac{I_C}{2\pi} \cdot \left[\frac{x-S}{(x-S)^2 + (y-h)^2} - \frac{x-S}{(x-S)^2 + (y+h)^2} \right] \end{aligned} \tag{28}$$

$$B_h = \mu_0 H_h \quad \text{and} \quad B_v = \mu_0 H_v \tag{29}$$

The magnetic field at the level of the earth and a distance x from the origin O of the axes (from the center of the line) will be calculated as follows taking $y = 0$:

$$H_{ht} = \frac{I_a}{2\pi} \frac{2h}{(x+S)^2 + h^2} + \frac{I_b}{2\pi} \frac{2h}{x^2 + h^2} + \frac{I_c}{2\pi} \frac{2h}{(x-S)^2 + h^2} \tag{30}$$

$$H_{vt} = 0 \tag{31}$$

So from formula (30), we can express the following geometric factors for the horizontal component:

$$\begin{cases} K_a = \dfrac{2h}{(x+S)^2 + h^2} \\ K_b = \dfrac{2h}{x^2 + h^2} \\ K_C = \dfrac{2h}{(x-S)^2 + h^2} \end{cases} \tag{32}$$

From formula (32) it can be shown that the modulus of the horizontal component of the magnetic field is equal to:

$$|H_{ht}| = \frac{I}{2\pi} \sqrt{K_a^2 + K_b^2 + K_C^2 - K_a K_b - K_b K_C - K_C K_a} \tag{33}$$

Finally, the horizontal component of the magnetic induction is easily deduced as follows:

$$|B_{ht}| = \mu_0 |H_{ht}| \cdot 10^6 \quad \text{in } (\mu\text{T}) \tag{34}$$

We replace the expression (33) with (34), and we find:

$$|B_{ht}| = \frac{I}{2\pi} \cdot 10^6 \sqrt{K_a^2 + K_b^2 + K_C^2 - K_a K_b - K_b K_C - K_C K_a} \tag{35}$$

2.2. Electromagnetic Modeling of the Interactions between Waves and Human Biological Tissues

In Figure 5, R: represents the resistance in Ohm per meter [W·m^{-1}], G: conduc-

tance in [Oh·m^{-1}] per meter: L: inductance in micro Henry per meter [mH·m^{-1}], and C: Capacitance in Pico Faraday per meter [pF·m^{-1}] [4]. From a reliability point of view, this equivalent electronic circuit model reproduces with maximum precision the electrical behavior of biological tissue, without taking into account its internal structure. It also reduces the simulation time and gives the possibility to simulate complex systems like the one under study [16].

The model in **Figure 5** above makes it possible to indirectly obtain the mathematical expressions of the voltage $V(x, t)$ and the current $I(x, t)$ thus induced from the propagation impedance of the wave in involving the electrical parameters of the model (R, L, C, and G).

$$\frac{\partial V(x,t)}{\partial x} + RI(x,t) + L\frac{\partial I(x,t)}{\partial t} = 0 \tag{36}$$

$$\frac{\partial I(x,t)}{\partial x} + GV(x,t) + C\frac{\partial I(x,t)}{\partial t} = J(x,t) \tag{37}$$

The FDTD models [16] of the current and the voltage induced in the human body by the electromagnetic field radiated by the HV line resulting from Equations (38) and (39) are the following:

$$I_k^n = \left(\frac{L}{\Delta t} + \frac{R}{2}\right)^{-1}\left[\left(\frac{L}{\Delta t} - \frac{R}{2}\right)I_k^{n-1} - \left(\frac{V_{k+1}^n - V_k^n}{\Delta x}\right)\right], 1 \le k \le N_{bs} \tag{38}$$

$$V_k^n = \left(\frac{C}{\Delta t} + \frac{G}{2}\right)^{-1}\left[\left(\frac{C}{\Delta t} - \frac{G}{2}\right)I_k^{n-1} - \left(\frac{I_k^{n-1} - I_{k-1}^{n-1}}{\Delta x}\right)\right], 2 \le k \le N_{bs} \tag{39}$$

3. Simulation

3.1. Declaration of Parameters

In this part, we have taken into account the parameters of 220 kV [24] and 132 kV [25] HV lines to obtain geometric data for the estimation of exposure to 50 Hz electromagnetic fields. Analytical modeling has been carried out on several of the most sensitive levels of the human body, level 0 m, level 1 m, level 1.5 m, and level 1.8 m representing respectively the contact of the feet with the ground, the place of sexuality and the fetus of a pregnant woman, the cardiac system and medical implants (pacemakers, defibrillators, etc.), the last level is the brain and cochlear implants [25] (see **Figure 6** and **Figure 7**).

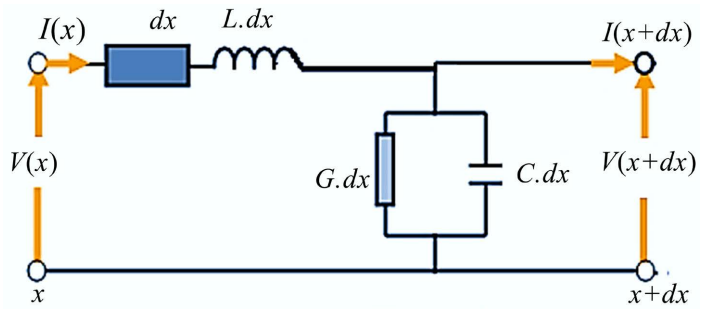

Figure 5. Equivalent electronic circuit of biological tissue [4] [16].

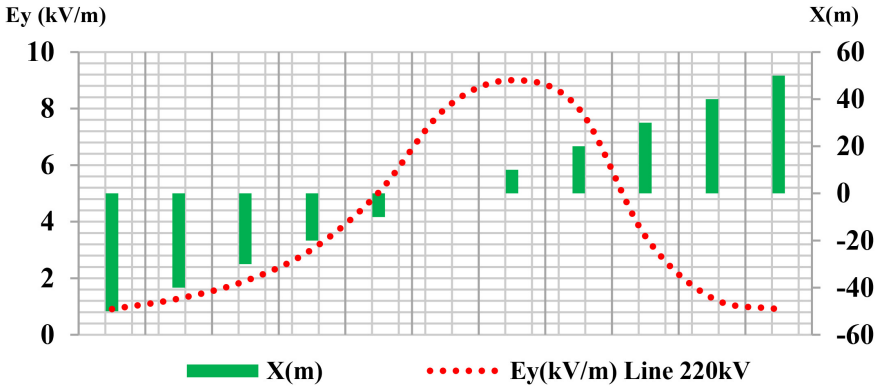

Figure 6. Intensity of the electric field generated by a 220 HV Line.

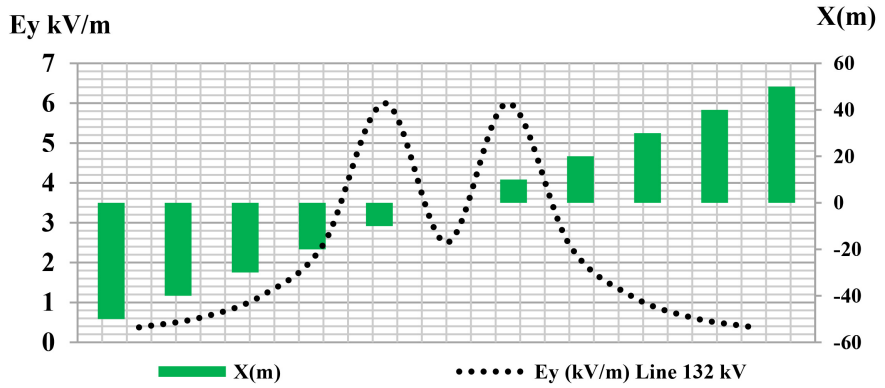

Figure 7. Intensity of the electric field generated by a 132 kV Line.

3.2. Results

By considering the frequency of 50 Hertz of propagation of electromagnetic waves in the vicinity of the 132 kV and 220 kV HV lines crossing the city of Kinshasa in DR Congo and the calculation codes developed above, the results of simulations of the electromagnetic environment of these HT lines are presented in Figures 6-14 below. Figure 8 and Figure 13 are respectively the results obtained experimentally in the work of (AHMIL INES and BELDI ASMA (2019)) [20] and (LIMANE Isamil Choayb and DJAHMI Aymen (2020)) [24].

3.3. Discussions

According to the curves in Figure 6 to Figure 7, the intensity of the electric field decreases by moving away from the axes of HV lines. Figure 6 shows that the intensity of the electric field takes the maximum value of 9 kV/m at the axis of the 220 kV HV line. Figure 7 demonstrates that the calculated electric field strength at ground level varies from point to point and that the maximum value of 6 kV/m is not in the middle of the line. These results can be compared with those obtained experimentally in the work of (AHMIL INES and BELDI ASMA (2019)) presented in Figure 8.

Figures 9-12 show the profile of the intensity of the magnetic field B generated by the 220 kV and 132 kV lines, it is observed that, for the 220 kV HV line,

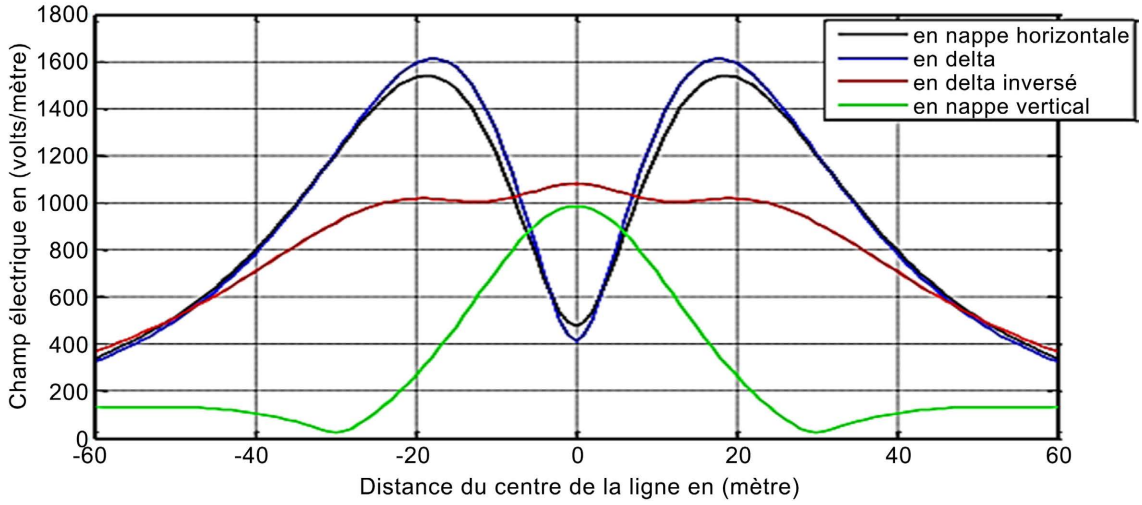

Figure 8. Intensity of the electric field generated by the four configurations. Results published by AHMIL INES and BELDI ASMA (2019) [20].

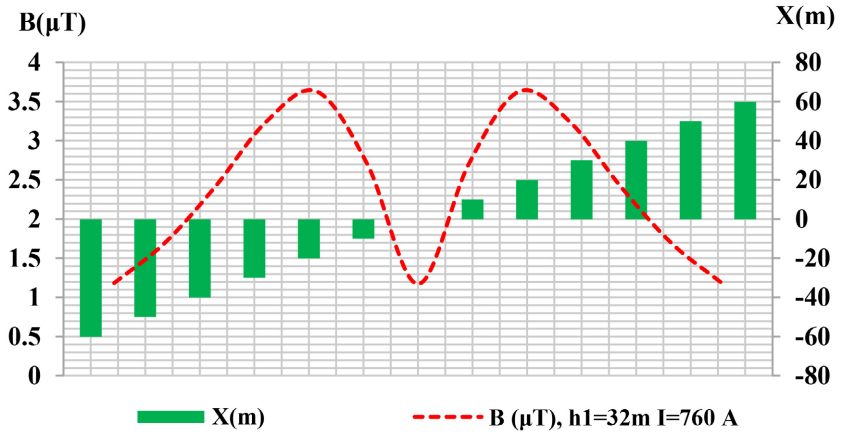

Figure 9. Intensity of the magnetic field generated by a 220 kV HV Line for h_1 = 32 m and I = 760 A.

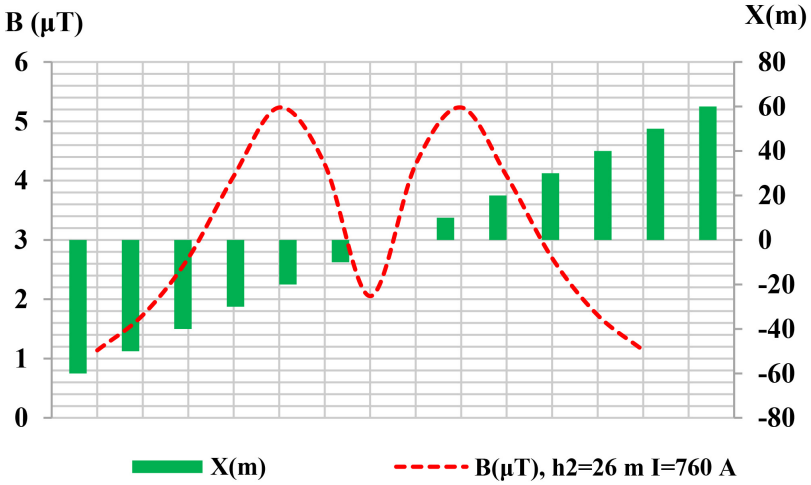

Figure 10. Intensity of the magnetic field generated by a 220 kV HV Line for h_2 = 26 m and I = 760 A.

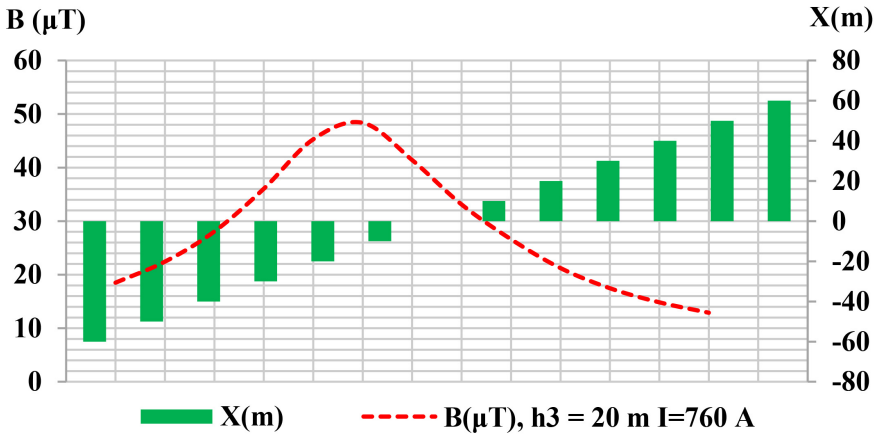

Figure 11. Intensity of the magnetic field generated by a 220 kV HV line for h_3 = 20 m and I = 760 A.

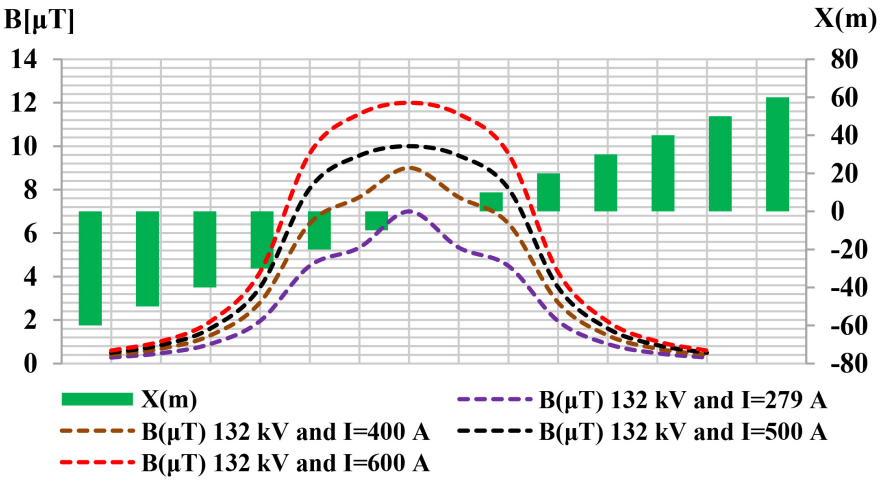

Figure 12. Intensity of the magnetic field generated by a 132 kV HV Line as a function of I = 279 A, 400 A, 500 A and 600 A.

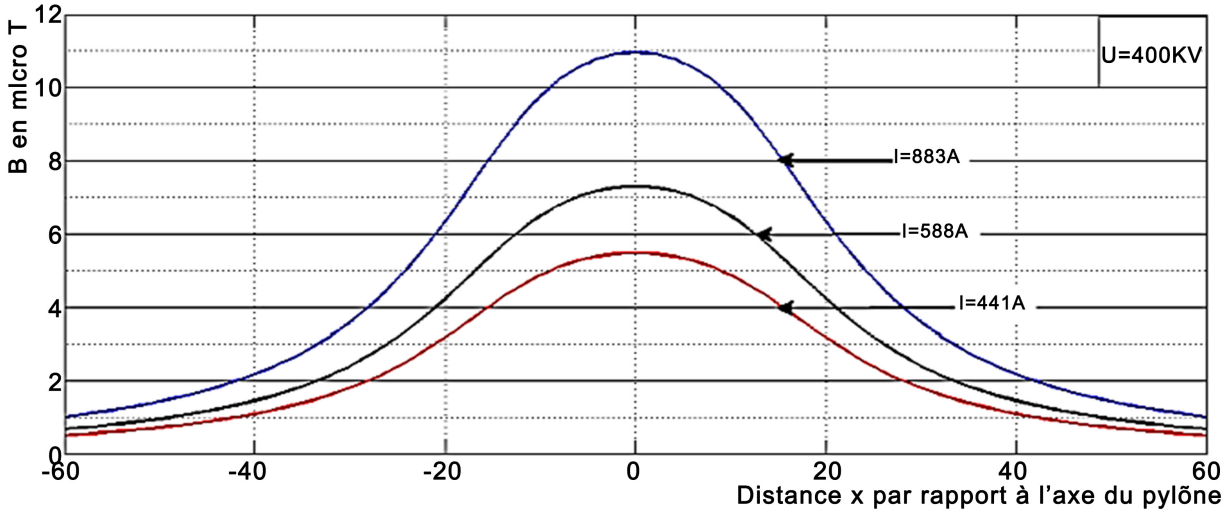

Figure 13. Intensity of the magnetic field generated by a 400 kV HV Line. Results published by LIMANE Isamil Choayb and DJAHMI Aymen (2020) [25].

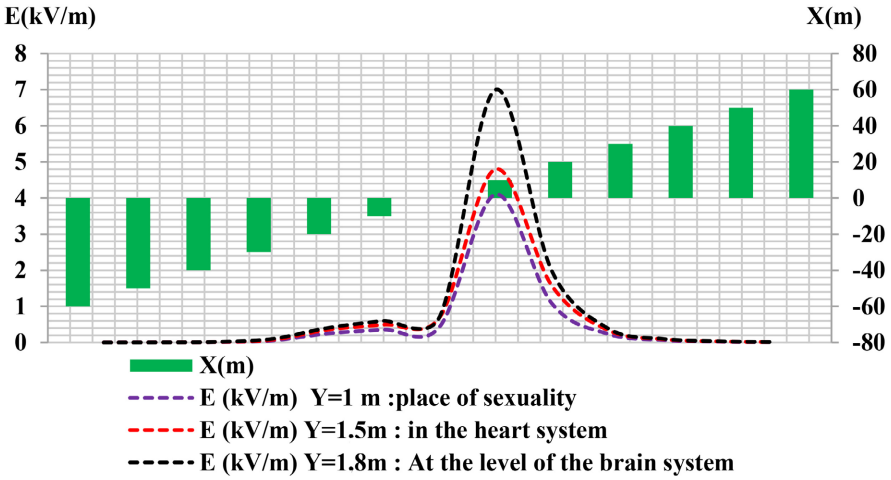

Figure 14. Electric field profiles generated by a 132 kV HV Line at the three most sensitive levels of the human body.

the maximum value of the magnetic field is 50 μT at the axis of the line, the intensity of the magnetic field increases with decreasing height and decreases away from the axis of the line. On the other hand, the profile of the magnetic field radiated by the 132 kV line is proportional to the current which crosses the line. The fractal dimensions of our simulations, however, confirm the results of Figure 13 obtained experimentally in the work of (LIMANE Isamil Choayb and DJAHMI Aymen (2020)). For approximately determined current values, we did not obtain values exceeding the ICNIRP limit (100 μT).

Figure 14 gives the estimate of exposure to the electric field in the vicinity of the 132 kV HV Line at several of the most sensitive levels of the human body. As we can notice, at the place of sexuality and the fetus of a pregnant woman, the maximum value of the electric field is about 4.1 kV/m, at the cardiac system, this field increases to 5 kV/m, and finally, at the level of the human brain, the exposure is at 7 kV/m despite this field decreasing when moving away from the HV line axis. We observe that the greatest electric field intensities are concentrated in the areas close to the conductors of the line. The field value at the cerebral level exceeds the safety guidelines established by the standards (5 kV/m).

4. Survey Data

Many questions arise about the impact of this HV equipment on the living conditions of residents living nearby, or even directly below. This is why we surveyed from March 02, 2019, to March 02, 2022, to check the living conditions of populations exposed to 132 kV and 220 kV HV lines in Kinshasa in the DR Congo to confirm the effects of EHV lines on the health. To this end, the data collected were analyzed using the two methods of Multiple Correspondence Analysis which allows a geometric visualization of the relationships significantly emerging between the different data and the Ascending Hierarchical Classification which makes it possible to group significantly by affinities, data varied in

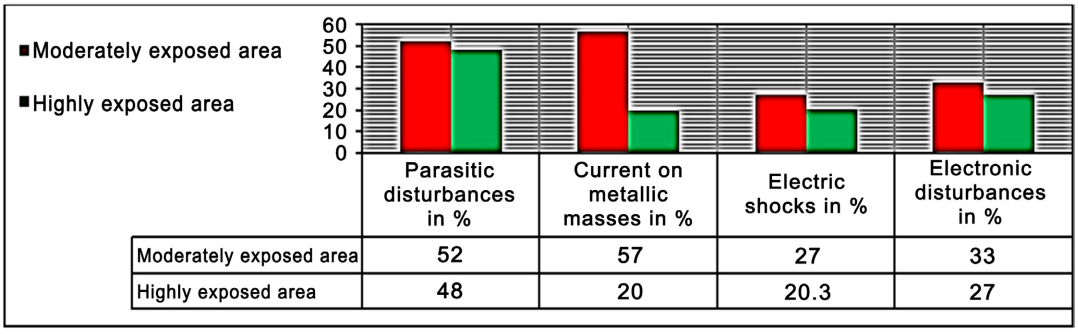

	Parasitic disturbances in %	Current on metallic masses in %	Electric shocks in %	Electronic disturbances in %
Moderately exposed area	52	57	27	33
Highly exposed area	48	20	20.3	27

Figure 15. Malfunctions of electrical or electronic devices in their home.

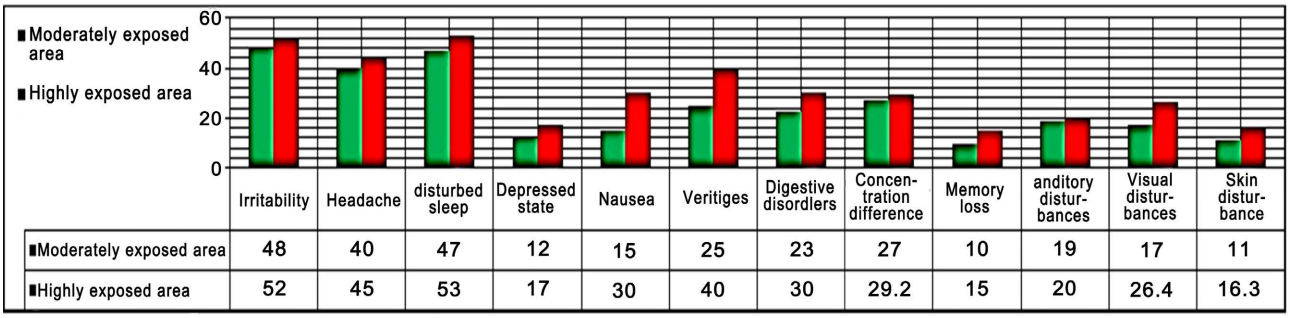

	Irritability	Headache	disturbed sleep	Depressed state	Nausea	Veritiges	Digestive disordlers	Concen-tration difference	Memory loss	anditory distur-bances	Visual distur-bances	Skin distur-bance
Moderately exposed area	48	40	47	12	15	25	23	27	10	19	17	11
Highly exposed area	52	45	53	17	30	40	30	29.2	15	20	26.4	16.3

Figure 16. The frequency of all the symptoms observed in the population residing near 132 kV and 220 kV HV Lines.

relationship with exposed populations, in the form of histograms of subordinate matches between them.

The results presented in Figure 15 and Figure 16 are statistically validated at the usual significance level ($\alpha = 0.05$). The statistical results are correlated by the exploitation of the data by the Analysis of Multiple Correspondences. The link between the frequency of symptoms and the fact of living near an HV line is very significant. It should be noted that this survey demonstrated certain facts in relation to the questions posed to the population such as irritation, headaches, sleep disturbance, depression, nausea, dizziness, digestive disorders, auditory and visual disturbances, skin disturbance, and malfunction of electrical or electronic devices in their homes.

5. Conclusions

Within the framework of this article, we studied the electromagnetic environment at the industrial frequency of 50 Hz in the vicinity of the electric lines HV. The goal is to systematize knowledge on the distribution of electric and magnetic field intensities under HV energy systems to predict the levels of public exposure to EM radiation emitted by them. To do this, the classical analytical method of the field produced near a high voltage line based on Maxwell's image theory, the Maxwell-Gauss and Maxwell-Ampère theorems was chosen and used to study the behavior lateral profiles of electric and magnetic fields emitted by 132 kV and 220 kV power lines with a view to their characterization as sources of electromagnetic disturbances. The 2D FDTD numerical formulation developed from

telegraphers' equations allowed us to model the influences of OEMs on living beings below and near HV lines. Various simulations carried out using computer tools illustrate the effects of the electrical and geometric parameters of pylons on the distribution of the electromagnetic field in the vicinity of HV lines.

The results obtained in the two cases studied, very high electric field values (6 kV/m for the 132 kV line and 9 kV/m for the 220 kV line) which exceed the safety instructions (5 kV/m), were visualized graphically. Regarding the distribution of the magnetic fields, and for approximately determined current values, we did not obtain values that exceed the limit of 100 μT as stipulated by the international standards in the matter. We observe that the greatest electric field intensities are concentrated in the areas close to the conductors of the line. For the exposure of a human being in perfect contact with the ground below or near a high-voltage line, the field value at the cerebral level exceeds the safety guidelines established by the standards. The fractal dimensions of our simulations, however, confirm the results obtained experimentally in the work published by other scientists working in this field.

Data from surveys carried out on the resident population below the 132 kV and 220 kV HV line crossing the city of Kinshasa in DR Congo have enabled us to note the risk associated with this radiation because some people complain of visual disturbances or fatigue but also a momentary weakness. After all, the link between the frequency of symptoms and the fact of living near an HT line is very significant.

In perspective, it would be interesting to study and develop 3D models and to study the effects of the electromagnetic field on a model simulating the dielectric characteristics of biological tissues. In addition, it is important to study the effects of the electromagnetic field for more complex situations such as the fields created by a transient transmission line. This study will be supplemented in the days to come by a survey which is carried out on the population living near the antennas of mobile telephone systems.

Conflicts of Interest

The author declares no conflicts of interest regarding the publication of this paper.

References

[1] Billel, A.R. (2016) Electromagnetic Compatibility: Study of the Electromagnetic Environment Generated by High-Voltage Lines. Master's Thesis, University 8 May 1945 Guelma Faculty of Science and Technology Department of Electrotechnical and Automatic Engineering, Guelma.

[2] National Research Council (U.S.) (2006) Possible Health Effects of Exposure to Resedentiel Electric and Magnetic Fields. National Academy Press, Washington DC.

[3] World Health Organization (WHO) (year) Framework for Developing Health-Based EMF Standards.

[4] Bassesuka Sandoka Nzao (2019-2022) Surveys Carried out on the Populations Liv-

ing below the High Voltage Lines Covering the City Province of Kinshasa. T*he Congolese Journal of Applied Technical Sciences*.

[5] Mimi, M. and Land, D.V. (1991) Measurement of Non-Resonant Disturbance of Antenna Electromagnetic Field Configurations for Biomedical Applications. *The Journal of Photographic Science*, **39**, 161-163. https://doi.org/10.1080/00223638.1991.11737141

[6] Nzao, A.B.S. (2021) Study and Modeling of Human Biological Tissue Exposed to High Frequency Electromagnetic Waves. *Open Journal of Applied Sciences*, **11**, 1109-1121. https://doi.org/10.4236/ojapps.2021.1110083

[7] Simicevic, N. and Haynie, D.T. (2005) FDTD Simulation of Exposure of Biological Material to Electro-Magnetic Nanopulses. *Physics in Medicine and Biology*, **50**, 347-360. https://doi.org/10.1088/0031-9155/50/2/012

[8] Wang, Y., Schimpf, P.H., Haynor, D.R. and Kim, Y. (1998) Geometric Effects on Resistivity Measurements with Four-Electrodeprobes in Isotropic and Anisotropic Tissues. *IEEE Transactions on Biomedical Engineering*, **45**, 877-884. https://doi.org/10.1109/10.686795

[9] Stuchly, M.A. and Dawson, T.W. (2000) Interaction of Low-Frequency Electric and Magnetic Fields with the Human Body. *Proceedings of the IEEE*, **88**, 643-664. https://doi.org/10.1109/5.849161

[10] Schoenbach, K.H., Xiao, S., Joshi, R.P., Camp, J.T., Heeren, T., Kolb, J.F. and Beebe, S.J. (2008) The Effect of Intense Subnanosecond Electrical Pulses on Biological Cells. *IEEE Transaction on Plasma Science*, **36**, 414-422. https://doi.org/10.1109/TPS.2008.918786

[11] Reivonen, S., Keikko, T., Isokorpi, J. and Korpinen, L. (1999) Internal Currents in a Human Body with Spheroidal Model in 400 kV Switching Substation. 11*th International Symposium on High-Voltage Engineering*, London, 23-27 August 1999, 31-34. https://doi.org/10.1049/cp:19990588

[12] Miranda, P.C., Hallett, M. and Basser, P.J. (2003) The Electric Field Induced in the Brain by Magnetic Stimulation: A 3-D Finite Element Analysis of the Effect of Tissue Heterogeneity and Anisotropy. *IEEE Transactions on Biomedical Engineering*, **50**, 1074-1085. https://doi.org/10.1109/TBME.2003.816079

[13] Raicu, V., Kitagawa, N. and Irimajiri, A. (2000) A Quantitative Approach to the Dielectric Properties of the Skin. *Physics in Medicine & Biology*, **45**, L1-L4. https://doi.org/10.1088/0031-9155/45/2/101

[14] Galeev, A.L. (2000) The Effects of Microwave Radiation from Mobile Telephones on Human and Animals. *Neuroscience and Behavioral Physiology*, **30**, 187-194. https://doi.org/10.1007/BF02463157

[15] Matsumoto, T., Chiba, A., Hayashi, N. and Isaka, K. (1999) Effect of Competitor ELF Electric and Magnetic Fields on Induced Current Density in Biological Model in the Vicinity of the Ground. 11*th International Symposium on High-Voltage Engineering*, London, 23-27 August 1999, 3. https://doi.org/10.1049/cp:19990587

[16] Nzao, A.B.S. (2022) Analysis and FDTD Modeling of the Influences of Microwave Electromagnetic Waves on Human Biological Systems. *Open Journal of Applied Sciences*, **12**, 912-929. https://doi.org/10.4236/ojapps.2022.126063

[17] Nzao, A.B.S. (2022) Analysis, Sources and Study of the Biological Consequences of Electromagnetic Pollution. *Open Journal of Applied Sciences*, **12**, 2096-2123. https://doi.org/10.4236/ojapps.2022.1212145

[18] Malik, N.H. (1989) A Review of the Charge Simulation Method and Its Applications. *IEEE Transactions on Electrical Insulation*, **24**, 3-20.

https://doi.org/10.1109/14.19861

[19] Garg, R. (2008) Analytical and Computational Methods in Electromagnetics. Artech House, London.

[20] Ines, A. and Asma, B. (2019) Analytical Modeling of Electromagnetic Fields in View of Estimation of Low Public and Professional Exposure Frequency. Master's Thesis, University of Badji Mokhtar-Annaba. https://biblio.univ-annaba.dz/ingeniorat/wp-content/uploads/2019/10/Ahmil-Ines-Beldi-Asma.pdf

[21] Begamudre, R.D. (2006) Extra High Voltage AC Transmission Engineering. 3 ème édition, New Age International Publishers, New Delhi.

[22] Denno, K. (2018) High Voltage Engineering in Power systems. CRC Press, Boca Raton. https://doi.org/10.1201/9781351073219

[23] Mourad, D. (2016) Experimental and Theoretical Modeling of Electromagnetic Fields Radiated by High Voltage Power Lines. Master's thesis, University Badji Mokhtar, Annaba.

[24] Nzuru Nsekere, J.P. (2009) Contribution to the Analysis and Realization of the Earthing of the Electrical Installations in Tropical Regions. Master's Thesis, Université de Liège, Liège. https://docplayer.fr/19381336-Contribution-a-l-analyse-et-a-la-realisation-des-mises-a-la-terre-des-installations-electriques-dans-les-regions-tropicales.html

[25] Choayb-Djahmi Aymen, L.I. (2020) Calculation of Electric and Magnetic Fields near Very High Voltage Lines. Master's Thesis, University May 8, 1945 Guelma, Guelma.